DOI: 10.1002/chem.200701764

Ionic Liquids of Bis(alkylethylenediamine)silver(I) Salts and the Formation of Silver(0) Nanoparticles from the Ionic Liquid System

Masayasu Iida,*[a] Chihiro Baba,[a] Michiko Inoue,[a] Hibiki Yoshida,[a] Eiji Taguchi,[b] and Hirotoshi Furusho[b]

Abstract: We have prepared novel ionic liquids of bis(*N*-2-ethylhexylethylenediamine)silver(I) nitrate ([Ag(eth-hex-en)$_2$]NO_3 and bis(*N*-hexylethylenediamine)silver(I) hexafluorophosphate ([Ag(hex-en)$_2$]PF_6), which have transition points at −54 and −6 °C, respectively. Below these transition temperatures, both the silver complexes assume amorphous states, in which the extent of the vitrification is larger for the eth-hex-en complex than for the hex-en complex. The diffusion coefficients of both the complex cations, measured between 30 (or 35) and 70 °C, are largely dependent on temperature; the dependence is particularly large in the case of the eth-hex-en complex cation below 40 °C. Small-angle X-ray scattering studies showed that the bilayer structure of the metal complex is formed in the liquid state for both the silver complexes. A direct observation of the yellowish [Ag(eth-hex-en)$_2$]NO_3 liquid by transmission electron microscopy (TEM) indicates the presence of nanostructures, as a microemulsion, of less than 5 nm. Such structures were not clearly observed in the [Ag(hex-en)$_2$]PF_6 liquid. Although the [Ag(eth-hex-en)$_2$]NO_3 liquid is sparingly soluble in bulk water, it readily incorporates a small amount of water up to [water]/[metal complex] = 7:1. Homogeneous and uniformly sized silver(0) nanoparticles in water were created by the reduction of the [Ag(eth-hex-en)$_2$]NO_3 liquid with aqueous $NaBH_4$, whereas silver(0) nanoparticles were not formed from the [Ag(hex-en)$_2$]PF_6 liquid in the same way.

Keywords: amines · electron microscopy · ionic liquids · nanostructures · silver

Introduction

Metallosurfactants and metallomesogens provide unique and functional aggregates not attainable in conventional organic surfactant systems.[1–10] Systematic studies are required to clarify the relationship between the molecular structures and the unique morphologies of the molecular assemblies. Ethylenediamine is one of the most common ligands in the history of metal complexes, and thus alkylethylenediamines are regarded as typical ligands for metallosurfactants. Because of the relatively simple structure of the alkylethylenediamine ligand among metallosurfactants, a series of alkylethylenediamine–metal complexes is suitable for systematic studies into the morphology of aggregates based on the molecular structure.

A variety of alkylethylenediamine metal complexes have been synthesized, and highly ordered aggregation systems in solution, such as microemulsions and lyotropic liquid crystals, have been investigated.[2,7–10] From these studies, we reported the synthesis of bis(*N*-alkylethylenediamine)silver(I) nitrate (alkyl = hexadecyl, dodecyl, octyl, and hexyl) and the X-ray crystallographic analysis of the dodecyl complex. Furthermore, the characteristic aggregation behavior of the dodecyl and octyl complexes in liquid-crystalline states and solution were also investigated.[9g,10a] In the latter study, bis(*N*-octylethylenediamine)silver nitrate had a transition point from the crystalline state to the thermotropic liquid crystalline state at 48 °C. The preparation of bis(*N*-hexylethylenediamine)silver(I) nitrate was also reported therein, but this complex does not assume a liquid-crystalline phase; thus, the physical properties, such as its melting point of 44 °C, were not described. These low-melting points for the ionic crystals mean that ionic liquids or ionic liquid crystals form

[a] Prof. M. Iida, C. Baba, M. Inoue, H. Yoshida
Department of Chemistry
Nara Women's University
Kita-uoya-nishi-machi, Nara 630–8506 (Japan)
Fax: (+81) 742-20-3397
E-mail: iida@cc.nara-wu.ac.jp

[b] E. Taguchi, H. Furusho
Research Center for Ultra-high Voltage Electron Microscopy
Osaka University, Yamada-oka
Suita, Osaka 565–0871 (Japan)

 © 2008 Wiley-VCH Verlag GmbH & Co. KGaA, Weinheim WILEY InterScience DISCOVER SOMETHING GREAT

above 50 °C. On the other hand, monoalkylamine silver complexes have been reported to have low melting points.[11] Furthermore, the formation of room-temperature ionic liquids of analogous monoalkylaminesilver trifluoromethanesulfonimide complexes has recently been reported, and these novel complexes were used as new electrolytes for electrodeposition.[12]

Herein, we have tried to lower the melting point of bis(*N*-hexylethylenediamine)silver(I) nitrate ($[Ag(hex\text{-}en)_2]NO_3$) by using molecular design to create room-temperature ionic liquids. As a result, bis(*N*-2-ethylhexylethylenedimaine)silver nitrate ($[Ag(eth\text{-}hex\text{-}en)_2]NO_3$), containing a small amount of water ($0.3\,H_2O$), and bis(*N*-hexylethylenediamine)silver hexafluorophosphate anhydride ($[Ag(hex\text{-}en)_2]PF_6$) assumed liquid states at room temperature, and their unique physical and chemical properties were elucidated (see Scheme 1 for the molecular structures). The displacement of the *N*-hexylethylenediamine ligand by *N*-2-ethylhexylethylenedimaine significantly lowers the melting point, even for the nitrate salt, and the structure in the solid state is amorphous. Although these silver(I) complexes are sparingly soluble in bulk water, $[Ag(eth\text{-}hex\text{-}en)_2]NO_3$ readily incorporates a small amount of water, and the properties of the silver complex depend significantly on the amount of water present ($W_0 = [H_2O]/[Ag\ complex]$).

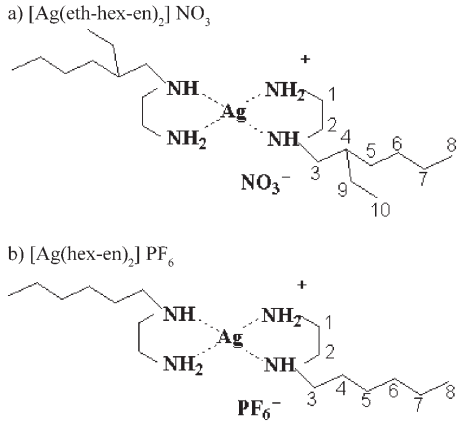

Scheme 1. Molecular structures of a) $[Ag(eth\text{-}hex\text{-}en)_2]NO_3$ and b) $[Ag(hex\text{-}en)_2]PF_6$.

We based this study into the formation of the ionic liquids on a series of bis(alkylethylenediamine)silver(I)-type complexes for the following reasons: A slight change in the molecular structure of these silver complexes offers a variety of molecular assemblies at ambient temperature,[9g] and the formation of ionic liquids can be considered to be a category of molecular-assembly systems. Furthermore, it is characteristic that the amphiphilic metal complexes with double alkyl chains provide metal nanoparticles from the reversed-micellar or water-in-oil (W/O) microemulsion system in a high yield.[10,13] We, thus, tried to create silver nanoparticles from the present ionic liquid systems by using reduction and directly observed the nanostructures of the ionic liquids through transmission electron microscopy (TEM) by monitoring the silver(0) particles. The shape and size of the silver(0) nanoparticles should provide useful information concerning the microstructure of the ionic liquids.

Results and Discussion

Solubilities of the silver complexes in various solvents: The newly prepared $[Ag(eth\text{-}hex\text{-}en)_2]NO_3$ complex is hardly soluble in bulk water but incorporates water up to $W_0 = 7$ to form homogeneous and transparent solutions. An increase in the water content makes the liquid more fluid, as described below in the diffusion studies. The $[Ag(hex\text{-}en)_2]PF_6$ liquid is also insoluble in water, which is different from the corresponding nitrate salt.[9g] Both the metal complex liquids readily dissolve in many organic solvents. Before investigating the physical properties in detail, we verified their solubilities in various solvents and classified them into three categories: 1) more than 10 % (w/v), 2) between 0.1–10 % (w/v), and 3) less than 0.1 % (w/v; Table 1).

The decomposition of $[Ag(eth\text{-}hex\text{-}en)_2]NO_3$ in certain polar organic solvents reflects the strong solvation at the head group. This complex is readily soluble in many organic solvents, other than CH_3Cl, which is favorable for the purification. The larger hydrophobicity of $[Ag(hex\text{-}en)_2]PF_6$ than $[Ag(hex\text{-}en)_2]NO_3$ can be attributed to the lesser hydration of the PF_6^- ion than the NO_3^- ion and/or to the specific molecular interactions between the metal complex cations and the counterions.

Changes in the ^{13}C NMR spectra through complex formation: The ^{13}C NMR spectra for the $[Ag(eth\text{-}hex\text{-}en)_2]NO_3$ and $[Ag(hex\text{-}en)_2]PF_6$ liquids are shown in Figure 1. The high viscosity of the former complex makes the signals broadened (the line-widths are 50–100 Hz for the alkyl chains and head groups, respectively) The assignment of each signal was performed based on ^{13}C–^1H COSY 2D NMR analysis in benzene, measurement of the ^{13}C NMR T_1

Table 1. A classification[a] of the solubilities of the (alkylethylenediamine)silver(I) complexes.

	Water	DMSO	DMF	Methanol	Ethanol	Acetone	Dichloro-methane	Ethyl acetate	$CHCl_3$	Diethyl ether	Benzene	Dioxane	Cyclo-hexane
$[Ag(hex\text{-}en)_2]NO_3$	1	1	1	1	1	1	1	1	2	3	3	1	1
$[Ag(hex\text{-}en)_2]PF_6$	3	1	1	1	1	1	1	1	3	3	1	1	1
$[Ag(oct\text{-}en)_2]NO_3$	3	1	1	3	3	1	1	1	2	2	1	1	3
$[Ag(eth\text{-}hex\text{-}en)_2]NO_3$	3	X	X	1	1	1	1	1	3	1	1	1	1

[a] 1: >10 %; 2: 0.1–10 %; 3: <0.1 %, X: decomposed. DMF = *N*,*N*-dimethylformamide, DMSO = dimethyl sulfoxide.

 © 2008 Wiley-VCH Verlag GmbH & Co. KGaA, Weinheim

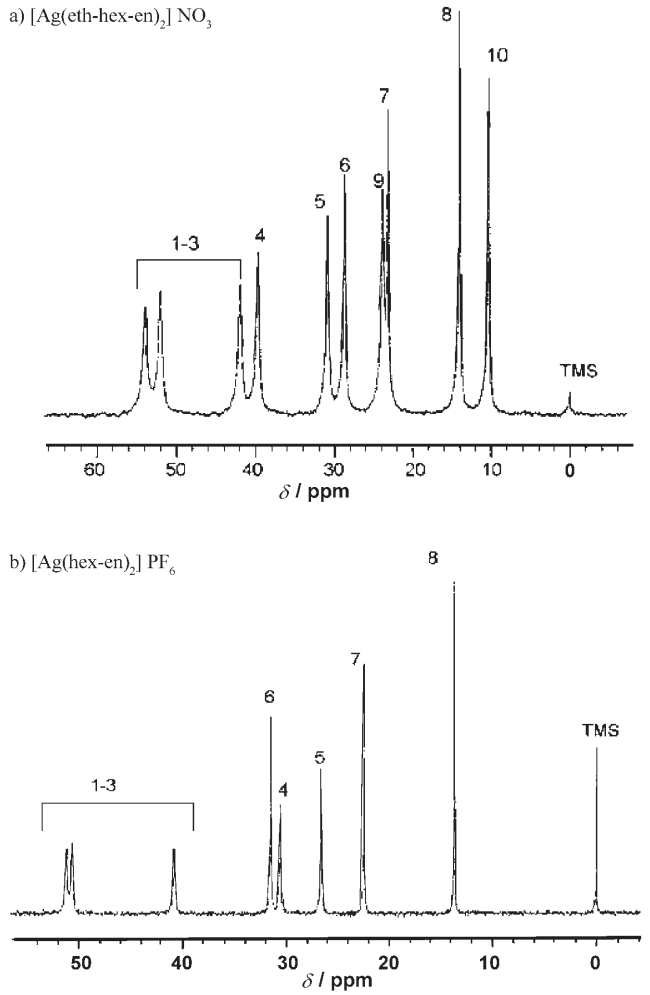

Figure 1. ^{13}C NMR spectra for the a) [Ag(eth-hex-en)$_2$]NO$_3$ and b) [Ag(hex-en)$_2$]PF$_6$ liquids. The numbering of each carbon atom is depicted in Scheme 1.

relaxation time, and reference to the assignment of analogous surfactants[14] (Figure 1). The ^{13}C NMR T_1 values at 27 °C for each signal of [Ag(eth-hex-en)$_2$]NO$_3$ and [Ag(hex-en)$_2$]PF$_6$ in [D$_6$]benzene (5 %) were as follows: [Ag(eth-hex-en)$_2$]NO$_3$: 1.63 s (δ = 10.49 ppm for C10); 2.73 s (δ = 14.10 ppm for C8); 1.53 s (δ = 23.26 ppm for C7); 370 ms (δ = 23.98 ppm for C9); 650 ms (δ = 28.82 ppm for C6); 350 ms (δ = 31.01 ppm for C5); 470 ms (δ = 39.94 ppm for C4); 170 ms (δ = 42.02 ppm); 160 ms (δ = 52.14 ppm); 273 ms (δ = 54.10 ppm). [Ag(hex-en)$_2$]PF$_6$: 3.69 s (δ = 13.94 ppm for C8); 2.88 s (δ = 22.69 ppm for C7); 1.34 s (δ = 26.82 ppm for C5); 960 ms (δ = 30.85 ppm for C4); 1.87 s (δ = 31.78 ppm for C6); 403 ms (δ = 40.68 ppm); 551 ms (δ = 50.62 ppm); 405 ms (δ = 50.98 ppm). A discrimination of signals from C1–C3 in the head group was not performed. We compared the changes in the ^{13}C NMR chemical shifts of the ligands between the free ligand and that of the silver complex in neat liquid and 5 % solutions of benzene (Table 2).

To distinguish the changes in the chemical shifts of the signals from the ligands by complexation between the coordination to the silver center and the intermolecular interactions in the ionic liquid system, we compared the changes in chemical shift between the neat state and samples in a 5 % solution in benzene. For both the alkylethylenediamine systems in benzene, the changes in the chemical shifts of the terminal carbon atoms (C8 and C7 for both the complexes) through complexation with the silver center are only slight but are large for the carbon atoms in the head group region (C1–C3). On the other hand, the complexation in the neat systems causes larger changes in the chemical shift than in benzene for many signals, particularly in the case of the terminal carbon atoms. The difference in the effect of the complexation on the chemical shifts, depending on the carbon position, is appropriately estimated by taking the ratio of the change in the chemical shift $\Delta\delta$ as a result of the complexation in neat liquid to the change in benzene for each signal.

The results are listed in Table 2 for each system. In the case of the carbon atoms in the head group (C1–C3), the changes in the chemical shift as a result of the complexation are relatively large, even in benzene, whereas in the ionic liquid systems both the intra- and intermolecular interactions from the complexation will cooperatively affect the change in the chemical shift; thus, the estimated ratios are hard to clearly interpret. On the other hand, the changes in the chemical shift of the signals from the alkyl chains can be more clearly explained: In the hex-en system, the magnitude of the ratios of the carbon atoms in the alkyl chains follow a trend in the order C7 > C8 $\gg$ C6 > C5 > C4 (absolute value). In the eth-hex-en system, there is a trend that follows in a similar manner to the hex-en complex, although it is less clear, that the terminal C8 and C7 carbon atoms show significantly larger changes in neat liquid than in benzene. These results for both systems indicate that in the formation of the ionic liquids the entanglement of the alkyl chains is important for self-aggregation (namely, the ionic liquids) of the silver complex cations. The short-range molecular interactions monitored by the chemical shifts of the signals from the terminal C8 and C7 carbon atoms show significantly larger changes in neat liquid than in benzene. The short-range molecular interactions monitored by the changes in the chemical shifts are more complicated in the eth-hex-en complex than in the hex-en complex.

Self-diffusion and electric conductivity: The [Ag(eth-hex-en)$_2$]NO$_3$ liquid is very viscous at ambient temperature, whereas it becomes fluid like normal liquids above 40 °C. The dynamic properties of the liquids were quantitatively studied by self-diffusion measurements of the silver complex cations ([Ag(eth-hex-en)$_2$]$^+$ and [Ag(hex-en)$_2$]$^+$) and the contained water in the [Ag(eth-hex-en)$_2$]NO$_3$ system by using ^{1}H NMR pulsed-field gradient (PFG) spectroscopic analysis. The diffusion coefficients as a function of temperature are given by Arrhenius plots, as shown in Figure 2, in which the dependence of the diffusion coefficients on the water content W_0 for [Ag(eth-hex-en)$_2$]NO$_3$ is also depicted. As a result of the limitation of the power of our machine,

 © 2008 Wiley-VCH Verlag GmbH & Co. KGaA, Weinheim

Table 2. Changes in the ^{13}C NMR chemical shifts through the formation of silver complexes

eth-hex-en system					hex-en system				
Chemical shift [ppm]		Complexation	Δ(neat)/	Assignment	Chemical shift [ppm]		Complexation	Δ(neat)/	Assignment
eth-hex-en	silver complex	Δ	Δ(benzene)		hex-en	silver complex	Δ	Δ(benzene)	
				Neat					
10.713	10.227	−0.486	1.2	10	14.089	13.622	−0.467	23	8
14.079	13.913	−0.166	−2.9	8	22.934	22.418	−0.516	29	7
23.245	23.054	−0.191	−2.8	7	27.41	26.622	−0.788	2.8	5
24.355	23.77	−0.585	1.0	9	30.63	30.592	−0.038	−0.08	4
29.113	28.64	−0.473	1.5	6	32.187	31.496	−0.691	9.0	6
31.389	30.845	−0.544	1.2	5	42.083	40.847	−1.236	0.98	1–3
39.358	39.624	0.266	1.6	4	50.149	50.645	0.496	0.64	
41.324	41.887	0.563	2.7		53.195	51.19	−2.005	1.2	
52.737	52.015	−0.722	0.96	1–3					
52.951	53.891	0.94	0.78						
				5% solution in benzene					
10.907	10.489	−0.418		10	13.963	13.943	−0.02		8
14.041	14.099	0.058		8	22.71	22.692	−0.018		7
23.187	23.255	0.068		7	27.098	26.816	−0.282		5
24.559	23.975	−0.584		9	30.397	30.854	0.457		4
29.132	28.821	−0.311		6	31.856	31.779	−0.077		6
31.477	31.01	−0.467		5	41.947	40.682	−1.265		1–3
39.777	39.942	0.165		4	49.838	50.616	0.778		
41.81	42.015	0.205			52.708	50.976	−1.732		
52.893	52.144	−0.749		1–3					
	54.1	1.207							

the diffusion coefficients below $1.0\times10^{-12}\,m^2s^{-1}$ had larger experimental errors and, thus, are not described herein (the corresponding data are for the eth-hex-en complex of $W_0=0.3$ below 40 °C). Good linearities in the Arrhenius plots are shown for $[Ag(hex\text{-}en)_2]^+$ (Figure 2e) and for water at larger W_0 values (Figure 2b–d). On the other hand, the plots are largely curved for the $[Ag(eth\text{-}hex\text{-}en)_2]NO_3$ systems at lower W_0 values. The plot is particularly curved below 40 °C in the regions of the lower W_0 values.

The Vogel–Tamman–Fulcher (VTF) equation (1) was satisfactorily applied to describe the temperature dependence of the diffusion coefficients of ionic liquids:[15]

$$D = D_0 \exp\left(-\frac{B}{T-T_0}\right) \quad (1)$$

In the present systems, the parameters D_0, B, and T_0 were determined on the basis of Equation (1) (see Table 2). To estimate the fitted parameters, we first used the data for $[Ag(eth\text{-}hex\text{-}en)_2]NO_3$ in which $W_0=0.3$ and determined the best fitting parameter of T_0 as 200 K. This value was also used in the other systems for comparison, as the error of this value did not significantly affect the estimates of the R^2 values for the other systems. The D_0 and B values in certain systems with good linearities in the Arrhenius plots (Figure 2) were also determined to fit Equation (1) using the same T_0 value of 200 K for comparison.

Small diffusion coefficients of $[Ag(eth\text{-}hex\text{-}en)_2]^+$ at the lowest water content ($W_0=0.3$) mean the formation of strong self-assemblies of the complexes. Particularly, the liquid at room temperature is regarded as a super-cooling liquid. With an increase in the water content, the liquid becomes significantly more fluid and the diffusion coefficients of both $[Ag(eth\text{-}hex\text{-}en)_2]^+$ and water increase. It is remarkable that with an increase in the water content, the linearity of the Arrhenius plot becomes better. For the same T_0 value, both the D_0 and B values increase with an increase in the water content in the case of water, whereas they decrease in the case of $[Ag(eth\text{-}hex\text{-}en)_2]^+$ (these values slightly increase from $W_0=5$ to 6.5, which may be an experimental error; Table 3).

In the case of $[Ag(hex\text{-}en)_2]^+$, the liquid is more fluid and, thus, the diffusion coefficient is somewhat larger and the temperature dependence is smaller than for $[Ag(eth\text{-}hex\text{-}en)_2]^+$ (Figure 2e). It is characteristic that in the hex-en complex system, the linearity of the Arrhenius plot ($T_0=0$) is better than for the other cases and it is not necessary to use Equation (1).

Although both the silver complexes are stable when stored in a refrigerator, the colorless liquids become yellowish with an increase in temperature. However, the ^{13}C NMR spectrum was almost unchangeable (within a shift of $\Delta\delta=0$–0.05 ppm for each signal), and the CHN elemental analyses were coincident with the calculated values within 0.5%, despite the color change. We, thus, considered that the self-diffusion coefficients were not significantly affected by the color change at higher temperatures.

The electric conductivities were 31 and 74 $\mu S\,cm^{-1}$ for the $[Ag(eth\text{-}hex\text{-}en)_2]NO_3$ and $[Ag(hex\text{-}en)_2]PF_6$ liquids, respectively, whose values are very small, thus reflecting the high viscosities. Therefore, this type of ionic liquid will be disad-

 © 2008 Wiley-VCH Verlag GmbH & Co. KGaA, Weinheim

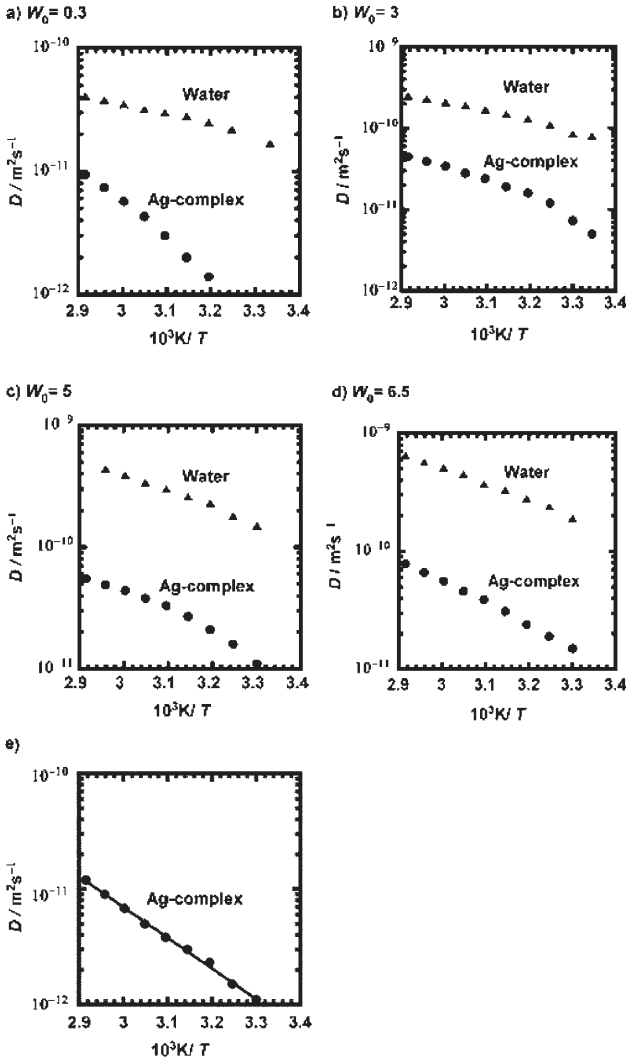

Figure 2. Diffusion coefficients of the eth-hex-en complex containing varying amounts of water (a–d) and the hex-en complex (e) as a function of temperature and shown as Arrhenius plots. In (a), no water was added. In the case of the eth-hex-en complex, the plots are drawn based on Equation (1) using $T_0 = 200$ K, and the values of D_0 and B given in Table 3. In the case of the hex-en complex, the plot is drawn by linear fitting.

vantageous for an application towards electrical conductivity.

DSC studies: The appearance of $[Ag(eth\text{-}hex\text{-}en)_2]NO_3$ as a solid at around −60 °C is transparent and glassy, whereas $[Ag(hex\text{-}en)_2]PF_6$ is devitrified in the solid state. The former glassy solid was confirmed to be isotropic by using polarizing microscopy (PM). The differential scanning calorimetry (DSC) curve for $[Ag(eth\text{-}hex\text{-}en)_2]NO_3$ is given in Figure 3a. The transition at −54 °C is like a glass transition. The small endothermic peak at around −30 °C in the DSC curve corresponds to an enthalpy change of around 1.5 kJ mol^{-1}, which is too small for the transition from the crystalline to isotropic liquid state; both the glassy transition profile and the small enthalpy change indicate that the solid is almost amorphous. For comparison, the $[Ag(hex\text{-}en)_2]NO_3$ crystal was a melt at 44 °C, and the DSC curve gives one sharp endothermic peak with an enthalpy change of 34 kJ mol^{-1} (Figure 3b).

In contrast to the $[Ag(eth\text{-}hex\text{-}en)_2]NO_3$ complex, the DSC curve for $[Ag(hex\text{-}en)_2]PF_6$ gives a sharp and simple endothermic peak that corresponds to an enthalpy change of 18 kJ mol^{-1} (Figure 3c). This value is appreciably larger than for the eth-hex-en complex but smaller than the melting enthalpies of crystalline $[Ag(hex\text{-}en)_2]NO_3$. The peak shape and value of the enthalpy change for $[Ag(hex\text{-}en)_2]PF_6$ suggest that the solid structure is more ordered than that for $[Ag(eth\text{-}hex\text{-}en)_2]NO_3$.

WAXS and SAXS studies: The wide-angle X-ray scattering (WAXS) profiles for $[Ag(eth\text{-}hex\text{-}en)_2]NO_3$ and $[Ag(hex\text{-}en)_2]PF_6$ at two temperatures (−58 and 25 °C) are shown in Figure 4a and b, respectively. The measurements for both complexes at −150 °C gave the same profiles (not depicted) as at −58 °C. Both the profiles show amorphous structures, whereas $[Ag(hex\text{-}en)_2]PF_6$ is less amorphous than $[Ag(eth\text{-}hex\text{-}en)_2]NO_3$ and several sharp peaks appear. The peak at $2\theta = 21°$ is attributed to typical methylene–methylene short-range interactions. The peak line-widths are 16° for the eth-hex-en complex and 10.5° for the hex-en complex both at 25 and −58 °C. This result means that the short-range ordering is higher for the hex-en complex. In the eth-hex-en complex, a very broad peak is otherwise present in the larger-angle region in both the liquid and solid states. The sharp peaks as a result of the crystalline portions appear more clearly in the hex-en complex. This structure causes a larger and simpler endothermic peak in the DSC curve relative to the eth-hex-en complex. The short-range structure of the hex-en complex is, thus, more ordered in the liquid state than in the eth-hex-en complex. The more complicated short-range structure for the eth-hex-en complex than for the hex-en complex observed from the WAXS measurements is consistent with the more complicated short-range interactions obtained from the ^{13}C NMR chemical shifts as described above.

As a series of the alkylethylenediaminesilver(I) complexes provide aggregates, such as microemulsions and thermotropic and lyotropic liquid crystals, it is anticipated that these complexes form an organized structure, which was investigated by small-angle X-ray scattering (SAXS) studies. The profiles in Figure 5 show that in both the systems similar broad peaks appear at $q = 3.2$ nm^{-1}, which corresponds to 2.0 nm d spacing. The half-width of the peak for $[Ag(eth\text{-}hex\text{-}en)_2]NO_3$ is 1.72°, whereas the half-width for $[Ag(hex\text{-}en)_2]PF_6$ is 2.47°, despite the same peak position. These values show the reverse relationship to that obtained from WAXS studies, that is, the nanostructure observed by SAXS studies is more ordered in the eth-hex-en complex than in the hex-en complex, whereas the nearby structure of the former complex is less ordered, as observed by WAXS studies.

 © 2008 Wiley-VCH Verlag GmbH & Co. KGaA, Weinheim

Table 3. Estimated values of D_0, B, and T_0 in Equation (1) for $[Ag(eth\text{-}hex\text{-}en)_2]^+$, H_2O, and $[Ag(hex\text{-}en)_2]^+$.

System	Species	T [°C]	T_0 [K]	$10^8 D_0$ [$m^2 s^{-1}$]	B [K]	$R^{2[a]}$
$[Ag(eth\text{-}hex\text{-}en)_2]NO_3$	silver complex cation	40–70	200	1.01	1030	0.999
(W_0=0.3)	water	35–70	200	0.027	270	0.998
			0	0.81	1800	0.997
$[Ag(eth\text{-}hex\text{-}en)_2]NO_3$	silver complex cation	30–70	200	0.32	610	0.999
(W_0=3)	water		200	0.32	360	0.999
			0	33	2450	0.996
$[Ag(eth\text{-}hex\text{-}en)_2]NO_3$	silver complex cation	30–70	200	0.30	560	0.997
(W_0=5)	water	30–70	200	1.03	440	0.999
			0	375	3050	0.997
$[Ag(eth\text{-}hex\text{-}en)_2]NO_3$	silver complex cation	30–70	200	0.56	610	1.000
(W_0=6.5)	water	30–70	200	1.44	445	0.999
			0	610	3100	0.998
$[Ag(hex\text{-}en)_2]PF_6$	silver complex cation	30–70	200	0.44	860	0.998
			0	53000	6100	0.999

[a] Square of the correlation coefficient.

To understand the SAXS peak positions for the present liquid systems, the molecular structure of $[Ag(dod\text{-}en)_2]NO_3$ (dod-en = *N*-dodecylethylenediamine) determined by X-ray crystallographic analysis[9g] is useful. The $[Ag(dod\text{-}en)_2]NO_3$ crystal was revealed to have a dinuclear structure, namely, the molecular composition unit is $[Ag_2(dod\text{-}en)_4](NO_3)_2$. Therefore, it is possible that $[Ag(hex\text{-}en)_2]NO_3$ and $[Ag(eth\text{-}hex\text{-}en)_2]NO_3$ also have a similar dinuclear composition to the dod-en complex in the liquid state. This molecular structure may cause the observed high viscosity. The X-ray crystallographic analysis of $[Ag_2(dod\text{-}en)_4](NO_3)_2$ showed that the size of the head group is 0.88 nm and the dodecyl chain length is 1.28 nm. These values give a molecular length of 3.44 nm for the dodecyl complex. The SAXS measurements for the $[Ag(dod\text{-}en)_2]NO_3$ liquid, on the other hand, revealed that the lamellar structure of 3.1 nm is formed in the thermotropic liquid crystals. A contraction of about 10% occurs through the transition from the crystalline to the liquid-crystalline state.

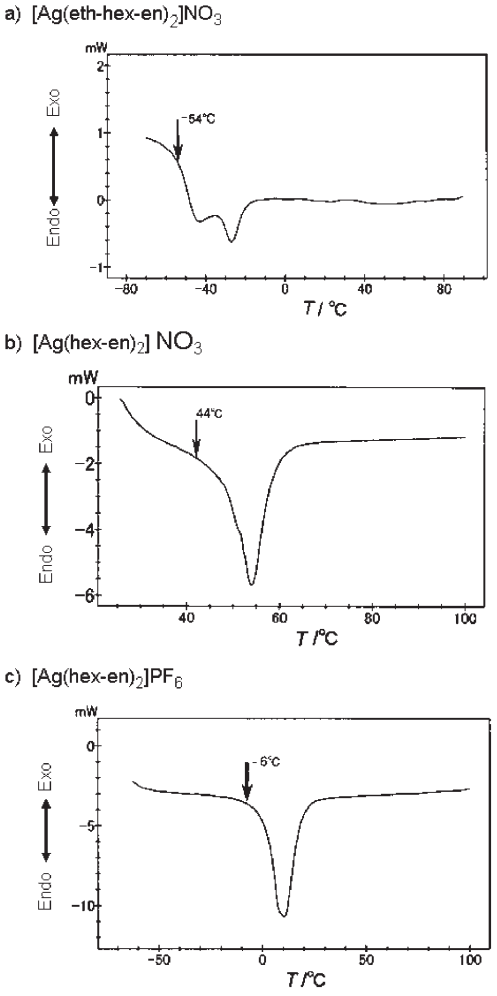

Figure 3. DSC curves of a) $[Ag(eth\text{-}hex\text{-}en)_2]NO_3 \cdot 0.3\,H_2O$ at −80–200 °C, b) $[Ag(hex\text{-}en)_2]NO_3$ at 25–100 °C, and c) $[Ag(hex\text{-}en)_2]PF_6$ at −80–200 °C.

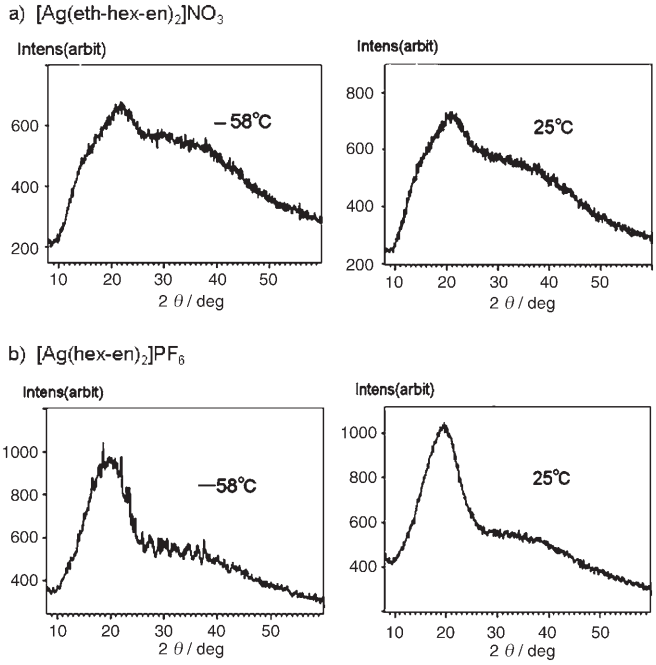

Figure 4. WAXS profiles of a) $[Ag(eth\text{-}hex\text{-}en)_2]NO_3 \cdot 0.3\,H_2O$ and b) $[Ag(hex\text{-}en)_2]PF_6$ at −58 and 25 °C.

© 2008 Wiley-VCH Verlag GmbH & Co. KGaA, Weinheim

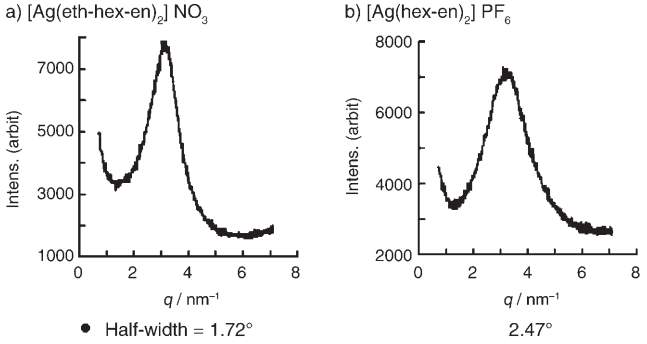

Figure 5. SAXS profiles of a) $[Ag(eth\text{-}hex\text{-}en)_2]NO_3 \cdot 0.3H_2O$ and b) $[Ag(hex\text{-}en)_2]PF_6$ at room temperature.

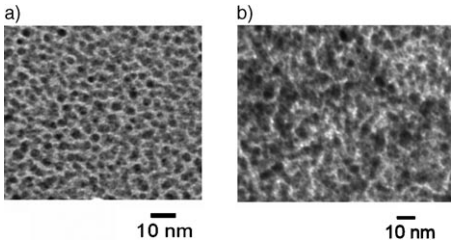

Figure 6. TEM images of the direct observation of a) $[Ag(eth\text{-}hex\text{-}en)_2]NO_3$ and b) $[Ag(hex\text{-}en)_2]PF_6$ in the liquid state.

In the present system, the molecular lengths of $[Ag(eth\text{-}hex\text{-}en)_2]^+$ and $[Ag(hex\text{-}en)_2]^+$ are estimated to be 2.16 nm by subtracting the C6 alkyl chains from the length of $[Ag(dod\text{-}en)_2]NO_3$. The SAXS peak at $q = 3.2\ nm^{-1}$ (corresponding to a d spacing of 2.0 nm) indicates that the contraction of about 10% of the bilayer occurs through the transition from the ideal crystalline state (an all *trans* conformation) to the ionic liquid states in a similar manner as the transition from the crystalline to the liquid crystalline states in the case of the dodecyl complex. Such nanostructures will be favorable in the formation of silver(0) nanoparticles from the liquids of these silver(I) complexes, as observed for the hexadecyl complex.

Observation of the nanostructures of the ionic liquids and the formation of silver(0) nanoparticles by treatment with aqueous $NaBH_4$: To obtain information on the nanostructure of the present ionic liquid system, we performed observations with TEM analysis by using two methods, namely, the direct observation of the ionic liquid system by monitoring reduced silver(0) particles produced by irradiation with an electron beam and the observation of silver(0) nanoparticles produced by reduction of the silver(I) complex in the liquid state with aqueous $NaBH_4$.

The silver complexes gradually became yellowish at room temperature as a result of the reduction of silver(I) to silver(0) ions, as described above.[16] This phenomenon was, on the other hand, useful to directly observe the nanostructure of the ionic liquid by monitoring the silver(0) particles. The ^{13}C NMR spectrum for $[Ag(eth\text{-}hex\text{-}en)_2]NO_3$ was almost unchanged by the slight coloration. We, thus, expect that the structure of the ionic liquids remain almost unchanged, even for the yellowish liquids. The transparent and colorless sample liquids were diluted to about one-third concentration with diethyl ether for $[Ag(eth\text{-}hex\text{-}en)_2]NO_3$ and with ethanol for $[Ag(hex\text{-}en)_2]PF_6$. These solutions were dried on carbon-coated copper grids and were directly observed by TEM studies. Figure 6a shows the TEM image for the yellowish (partially reduced) $[Ag(eth\text{-}hex\text{-}en)_2]NO_3$ liquid. This result indicates that the hydrophilic regions (black) and hydrophobic alkyl chain regions (white) present in the liquid state form organized structures, such as microemulsions. On the other hand, a similar TEM image for $[Ag(hex\text{-}en)_2]PF_6$ (Figure 6b) shows that the ordering structure is less clear. These TEM images are consistent with the results of the half-widths in the SAXS profiles, that is, in the case of the eth-hex-en complex, more ordered nanostructures are formed. A nanostructure, such as a W/O microemulsion, in the $[Ag(eth\text{-}hex\text{-}en)_2]NO_3$ liquid in the absence of an organic solvent is comparable to the W/O microemulsions of $[Ag(oct\text{-}en)_2]NO_3$ (oct-en = *N*-octylethylenediamine).[9g]

The reversed micelles or microemulsions composed of alkylethylenediaminesilver(I) and -palladium(II) complexes provide homogeneous and concentrated metal(0) nanoparticles by treatment with aqueous $NaBH_4$.[10] In the present liquid system, the silver ions are assembled in very limited nanoregions surrounded by the alkyl chains without organic solvents. Small amounts of water, strongly trapped in the metal complex, would be located in the hydrophilic moiety of the metal complex in the liquid state. The silver(I) ions are condensed in an appreciably greater density relative to common reversed micelles or W/O microemulsion systems. This property of ionic liquids containing metal ions suggests potential applications of the systems.[17] Thus, it is anticipated that it would be possible to effectively obtain silver(0) nanoparticles from the present ionic liquid system.

By the reaction of the $[Ag(eth\text{-}hex\text{-}en)_2]NO_3$ liquid with aqueous $NaBH_4$, a yellow sol with an absorption peak of 409 nm was obtained. The TEM images of the sol are shown in Figure 7. The $[Ag(eth\text{-}hex\text{-}en)_2]NO_3$ liquid gave well-uniformed nanoparticles relative to the $[Ag(hexdec\text{-}en)_2]NO_3$/*n*-heptane/water system (hexdec-en = *N*-hexadecylethylenediamine) despite the shorter alkyl-chain length.[10a] Only a small amount of water in the $[Ag(eth\text{-}hex\text{-}en)_2]NO_3$ liquid ($W_0 = 0.3$) would be favorable for the formation of monodispersed nanoparticles.

The effect of the addition of water on the formation of nanoparticles was investigated further. Although the $[Ag(eth\text{-}hex\text{-}en)_2]NO_3$ complex is sparingly soluble in water, this liquid can be homogeneously mixed with a small amount of water and results in a transparent liquid. With an increase in the water content, the liquid becomes more fluid. The $[Ag(eth\text{-}hex\text{-}en)_2]NO_3$ complex with varying W_0 values was treated with aqueous $NaBH_4$. A similar phenomenon as for the liquid with $W_0 = 0.3$ occurred and the resultant deep-yellow solution was observed by TEM analysis

 © 2008 Wiley-VCH Verlag GmbH & Co. KGaA, Weinheim

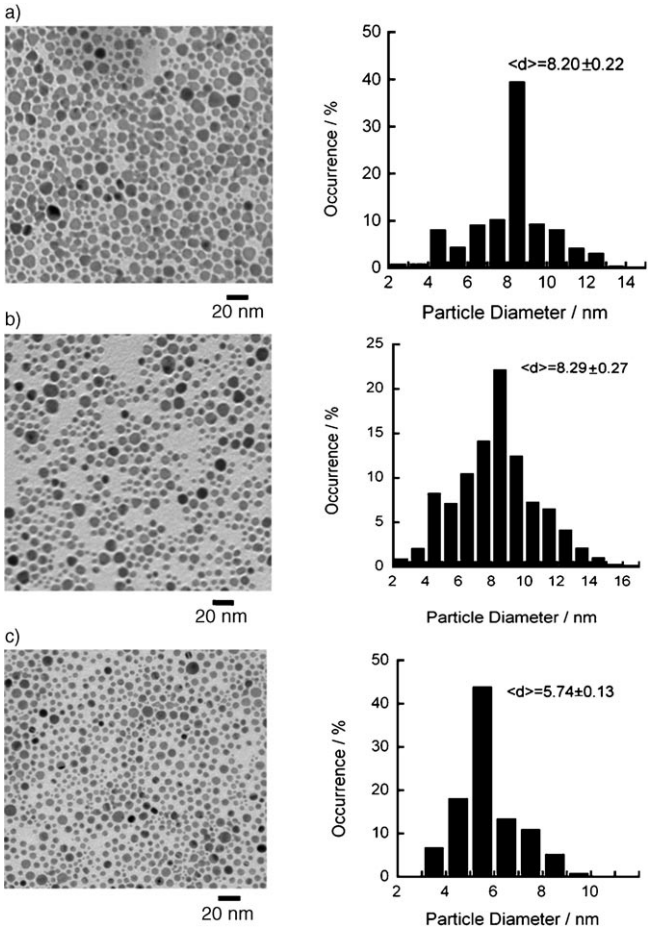

Figure 7. TEM images and size distribution of silver(0) nanoparticles obtained by the treatment of the various silver complex aggregate systems with aqueous $NaBH_4$. a) $[Ag(eth\text{-}hex\text{-}en)_2]NO_3{\cdot}0.3H_2O$ liquid; b) $[Ag(eth\text{-}hex\text{-}en)_2]NO_3$ ($W_0=5$) liquid; c) $[Ag(eth\text{-}hex\text{-}en)_2]NO_3{\cdot}0.3H_2O$ + eth-hex-en (molar ratio = 1:1) liquid.

after being dried on the carbon-film-coated copper grid. The sizes were somewhat larger and the distributions more polydispersed than those obtained from the liquid with $W_0=0.3$. Figure 7b shows a typical result for $W_0=5$.

To stabilize the reversed-micellar structure in the $[Ag(eth\text{-}hex\text{-}en)_2]NO_3$ liquid, we added further amounts of the ligand to the $[Ag(eth\text{-}hex\text{-}en)_2]NO_3$ liquid so that the ligand/solver molar ratio became 3:1. This liquid was treated with aqueous $NaBH_4$ solution in a similar manner to the 1:2 complex. The yellowish silver(0) sol was similarly obtained and observed by TEM analysis. In the TEM image, the silver(0) particles are a smaller size than in the neat system (Figure 7c), in which the particle sizes are uniform. This result indicates that the addition of the free ligand made the hydrophilic core of the aggregates smaller and stabilized the reversed-micellar structure.

In contrast to the $[Ag(eth\text{-}hex\text{-}en)_2]NO_3$ liquid, the reaction of the $[Ag(hex\text{-}en)_2]PF_6$ liquid with aqueous $NaBH_4$ gave only a colorless solution with precipitates of the silver metal. This contrasting behavior of the two silver(I) complexes is a result of the difference in the role of the ligands, that is, the silver(I) ion is effectively protected by the ligand against the aggregation of silver(0) particles in the reaction of the $[Ag(eth\text{-}hex\text{-}en)_2]NO_3$ liquid, whereas the ligands have no such effect in the $[Ag(hex\text{-}en)_2]PF_6$ liquid. This phenomenon is a result of the difference in the structures of the two kinds of ionic liquid (see Figure 6), namely, the ligands surround the silver(I) ions like oils in reversed-micellar structures in the eth-hex-en complex liquid, and the contact of the central silver(I) ion with the aqueous $NaBH_4$ is limited. This structure of the $[Ag(eth\text{-}hex\text{-}en)_2]NO_3$ liquid is favorable to incorporate a small amount of water and provides reaction fields of nanospace. The difference in the reaction with aqueous $NaBH_4$ between the two complexes is also compared to the difference in the solubilities in water, that is, when comparing the nitrate salts the eth-hex-en complex is sparingly soluble in water whereas the hex-en complex is readily soluble.

The results presented herein can be compared with those obtained from the analogous microemulsions comprising alkylethylenediamine–metal complexes, such as $[Ag(hexdec\text{-}en)_2]NO_3$/*n*-heptane/water and $[Pd(oct\text{-}en)_2]Cl_2/CHCl_3$/water systems.[10] The use of alkylethylenediamine–metal complexes for the formation of their metal(0) nanoparticles are useful to control the size distribution by changing the solution conditions, such as concentration and solvent. The longer alkyl chains will be more advantageous to obtain uniform silver(0) nanoparticles, because the hydrophilic core in the microemulsion system is better protected by the longer alkyl chains. However, the silver(0) nanoparticles obtained from the present ionic liquid system are more uniform, and the concentrations are higher than those obtained from the $[Ag(hexdec\text{-}en)_2]NO_3$/*n*-heptane/water microemulsions. This result also suggests that the alkyl chains of the $[Ag(eth\text{-}hex\text{-}en)_2]NO_3$ liquid will effectively protect the silver hydrophilic region and stabilize the ordered structure, such as reversed micelles. The change in the particle size with the addition of the ligand is also expected to develop this approach toward nanoparticle control.

It should be further emphasized that this method of preparing uniform-sized nanoparticles from an ionic liquid can be performed without organic solvents, namely, it is a green method.

Conclusion

Novel ionic liquids of silver complexes of 2-ethylhexylethylenediamine (eth-hex-en) and hexylethylenediamine (hex-en) have been isolated. In both the systems, the transition temperatures to the solid state are below 0 °C and the solid-state structures are amorphous.

In the formation of self-assembled ionic liquids, the important role of the terminal alkyl chains in the entanglement was clarified using ^{13}C NMR spectroscopic analysis. The entanglement of the alkyl chains was more clearly indicated in the hex-en complex than in the eth-hex-en complex. Organized nanostructures, such as W/O microemulsions, were

 © 2008 Wiley-VCH Verlag GmbH & Co. KGaA, Weinheim

formed and uniform-sized silver(0) nanoparticles were created by treatment with aqueous $NaBH_4$ in the case of the eth-hex-en complex, whereas the nanostructure was more disordered and silver(0) nanoparticles were not formed in the case of the hex-en complex.

Experimental Section

Materials: The $[Ag(eth\text{-}hex\text{-}en)_2]NO_3$ complex was synthesized by the treatment of $AgNO_3$ crystals (880 mg, 5.2 mmol) suspended in diethyl ether (15 mL) with 2-ethylhexylethylenedimaine ligand (1720 mg, 10 mmol) in diethyl ether (20 mL) at 0 °C. The eth-hex-en ligand was prepared according to the method for *N*-*n*-alkylethylenediamines.[18] After the reaction mixture was stirred overnight, the $AgNO_3$ crystals almost dissolved. The solution was filtrated and the diethyl ether was completely removed by a repeat freeze–thaw method to give a colorless and viscous liquid. The $[Ag(hex\text{-}en)_2]PF_6$ complex was obtained from the nitrate complex in ethanol by the addition of $NaPF_6$ with filtration of $NaNO_3$. The ethanol was removed by a repeated freeze–thaw method to give a colorless liquid. Elemental analysis (%) calcd for $[Ag(eth\text{-}hex\text{-}en)_2]NO_3{\cdot}0.3H_2O$: C 46.20, H 9.42, N 13.47; found: C 46.16, H 9.65, N 13.38; elemental analysis (%) calcd for $[Ag(hex\text{-}en)_2]PF_6$: C 35.50, H 7.45, N 10.35; found: C 35.58, H 7.56, N 10.58. The amount of water was determined as 0.30 mol and 0.05 mol per silver atom for $[Ag(eth\text{-}hex\text{-}en)_2]NO_3$ and $[Ag(hex\text{-}en)_2]PF_6$, respectively, by using a Karl–Fisher titration. We also used $[Ag(oct\text{-}en)_2]NO_3$ for comparison. This complex (crystals at room temperature) was prepared as previously reported.[9g]

Measurements: Transitions from the solid to liquid state and the loss of water from the solids were measured by differential scanning calorimetry (DSC; with Shimadzu DSC-50 attached LTC-50 apparatus for low-temperature measurements) at a constant rate of 10 K min^{-1} in the temperature range −80–200 °C. The samples (5–10 mg) were placed in aluminum pans and the measurements were recorded at a rate of 10 K min^{-1} under nitrogen at a flow rate of 50 cm^3 min^{-1}. Indium metal was used as the standard for temperature and enthalpy measurements. The WAXS studies were carried out at room temperature, −58, and −150 °C with a 0.8-kW generator of $Cu_{K\alpha}$ radiation (Panalytical X′Pert Pro). The intensity distribution of the WAXS studies was detected with a diode-array detector. The sample was put on the horizontal cell in vacuo (at around 7 Pa) and measured by using a reflection method. The SAXS was measured in the range $2\theta = 1$–$10°$ at room temperature with a 15-kW generator of $Cu_{K\alpha}$ radiation (Rigaku RINT-TTRIII). The intensity distribution of the SAXS was detected with a NaI scintillation counter. The sample was put in a 0.4-mm cell interposed by a 0.02-mm Mylar film (which had no peaks in the measured angle region). The SAXS profiles are given as plots of intensity versus q ($4\pi\sin\theta/\lambda$), in which $\lambda = 0.154$ nm.

The ^{13}C NMR spectra in solutions were recorded on a JEOL EX-270 FT NMR spectrometer operating at 67.9 MHz. The T_1 relaxation times for $[Ag(eth\text{-}hex\text{-}en)_2]NO_3$ were measured in $[D_6]$benzene by using an inversion recovery method. The dynamic properties of the silver complexes in the liquid state were studied by the measurement of self-diffusion of the silver complexes and the contained water (only for the $[Ag(eth\text{-}hex\text{-}en)_2]NO_3$ system) with varying W_0 values. The self-diffusion coefficients were measured by using ^1H NMR pulsed-field gradient (PFG) spectroscopic analysis with a JEOL FX-90 spectrometer operating at 90 MHz for the methylene chains in the silver(I) complex and water. The procedure has been described previously.[9e,g] The field gradient produced was up to around 0.9 T m^{-1}. The diffusion coefficients of the silver complexes and water were measured as a function of temperature and water content. The experimental errors in the diffusion coefficients of more than 2×10^{-12} m^2 s^{-1} were estimated to be less than 5%.

The electrical conductivity of the liquid was measured with a HORIBA B-173 machine for a small-scale sample by standardization with aqueous KCl (0.01 mol dm^{-1}; $\kappa = 1.41$ mS cm^{-1}; 25 °C).

The transmission electron microscopy (TEM) measurements were performed at ambient temperature on a Hitachi H-800 electron microscope operating at 200 kV. A specimen for the TEM measurements was prepared by spreading an ionic liquid or a small-drop colloidal solution directly onto a standard 200-mesh copper grid (coated with a thin amorphous carbon film) and letting the drop dry completely in air. The size distribution was derived from histograms for about 800 particles.

Preparation of silver(0) nanoparticles: The experimental procedure for the creation of silver(0) nanoparticles by treatment of the silver(I) complexes with $NaBH_4$ as a reducing agent is as follows: The $[Ag(eth\text{-}hex\text{-}en)_2]NO_3$ or $[Ag(hex\text{-}en)_2]PF_6$ liquids (1 g) were mixed with aqueous $NaBH_4$ (3 mL; 1.0 mol kg^{-1}); the amount of $NaBH_4$ added was in slight excess of the silver complex. The reaction mixture was stirred vigorously for about 2 h. A deep yellow solution was obtained with a black precipitate, which was removed by filtration. Dilution of the solution with water gave a yellow colloidal solution with a specific plasmon peak at 409 nm.

Acknowledgements

Part of this study was supported by the "Nanotechnology Support Project of the Ministry of Education, Culture, Sports, Science and Technology (MEXT), Japan" at the Research Center for Ultra-high Voltage Electron Microscopy (Osaka University, Japan). We are grateful to Mr. Yashiro at the Osaka Application Laboratory (Rigaku corporation) for carrying out the SAXS measurements and to Professor Toshiharu Suzuki at Nara Women's University for assistance with the WAXS measurements. This study was financially supported by a Nara Women's University Intramural Grant for Project Research.

[1] B. Donnio, *Curr. Opin. Colloid Interface Sci.* **2002**, *7*, 371.
[2] a) T. Sierra, *Metallomesogens* (Ed.: J. L. Serrano), VCH, Weinheim, **1996**; b) A. M. Giroud-Godquin in *Metal-Containing Liquid Crystals, Vol. 2B* (Eds: D. Demus, J. Goodby, G. W. Gray, H.-W. Spiess, V. Vill), Wiley-VCH, Weinheim, **1998**, Chap. 14; c) D. W. Bruce in *Inorganic Materials* (Eds: D. W. Bruce, D. O'Hare), Wiley, Chichester, **1996**, Chap. 8; d) D. W. Bruce, *Acc. Chem. Res.* **2000**, *33*, 831.
[3] a) K. Binnemans, C. Gorller-Walrand, *Chem. Rev.* **2002**, *102*, 2303; b) K. Binnemans, *Chem. Rev.* **2005**, *105*, 4148.
[4] P. C. Griffiths, I. A. Fallis, T. Chuenpratoom, R. Watanesk, *Adv. Biosci. Adv. Colloid Interf. Sci.* **2006**, *25*, 107.
[5] a) J. Bowers, M. J. Danks, D. W. Bruce, R. K. Heenan, *Langmuir* **2003**, *19*, 292; b) J. Bowers, M. J. Danks, D. W. Bruce, J. R. P. Webster, *Langmuir* **2003**, *19*, 299; c) J. Bowers, K. E. Amos, D. W. Bruce, *Langmuir* **2005**, *21*, 1346; d) J. Bowers, K. E. Amos, D. W. Bruce, R. K. Heenan, *Langmuir* **2005**, *21*, 5696.
[6] a) K. Santhakumar, N. Kumaraguru, S. Arunachalan, M. Arumugham, *Trans. Annu. Meet. Orthop. Res. Soc. Trans. Metal Chem.* **2006**, *31*, 62; b) N. Kumaraguru, S. Arunachalan, M. Arumugham, K. Santhakumar, *Trans. Annu. Meet. Orthop. Res. Soc. Trans. Metal Chem.* **2006**, *31*, 250.
[7] a) D. A. Jaeger, V. B. Reddy, N. Arulsamy, D. S. Bohle, D. W. Grainger, B. Berggren, *Langmuir* **1998**, *14*, 2589; b) N. Arulsamy, D. A. Jaeger, V. B. Reddy, N. Arulsamy, D. S. Bohle, D. W. Grainger, B. Berggren, *Inorg. Chem.* **2001**, *40*, 836; c) D. A. Jaeger, M. F. Peacock, D. S. Bohle, *Langmuir* **2003**, *19*, 4859.
[8] a) X. Lu, Z. Zhang, Y. Liang, *J. Chem. Soc. Chem. Commun.* **1994**, 2731; b) X. Lu, Z. Zhang, Y. Liang, *Langmuir* **1996**, *12*, 5501; c) X. Lu, Z. Zhang, Y. Liang, *Langmuir* **1997**, *13*, 533.
[9] a) M. Iida, A. Yonezawa, J. Tanaka, *Chem. Lett.* **1997**, 663; b) M. Iida, T. Tanase, N. Asaoka, A. Nakanishi, *Chem. Lett.* **1998**, 1275; c) M. Iida, H. Er, N. Hisamatsu, T. Tanase, *Chem. Lett.* **2000**, 518; d) Y. Ikeda, T. Imae, J.-C. Hao, M. Iida, T. Kitano, N, Hisamatsu, *Langmuir* **2000**, *16*, 7618; e) M. Iida, K. Asayama, S. Ohkawa, *Bull. Chem. Soc. Jpn.* **2002**, *75*, 521; f) H. Er, M. Iida, N. Asaoka, T. Imae, *Colloids Surf. A* **2003**, *221*, 119; g) M. Iida, M. Inoue, T. Tanase, T.

 © 2008 Wiley-VCH Verlag GmbH & Co. KGaA, Weinheim

Takeuchi, M. Sugibayashi, K. Ohta, *Eur. J. Inorg. Chem.* **2004**, 3920; h) H. Er, S. Ohkawa, M. Iida, *Colloids Surf. A* **2007**, *301*, 189.
[10] a) A. Manna, T. Imae, M. Iida, N. Hisamatsu, *Langmuir* **2001**, *17*, 6000; b) M. Iida, S. Ohkawa, H. Er, N. Asaoka, H. Yoshikawa, *Chem. Lett.* **2002**, 1050.
[11] A. C. Albeniz, J. Barbera, P. Espinet, M. C. Lequerica, A. M. Levelut, F. J. Lopez-Marcos, J. L. Serrano, *Eur. J. Inorg. Chem.* **2000**, 133.
[12] J.-F. Huang, H. Luo, S. Dai, *J. Electrochem. Soc.* **2006**, *153*, J9.
[13] I. Capek, *Adv. Colloid Interface Sci.* **2004**, *110*, 49.
[14] a) Y. Chevalier, C. Chachaty, *Colloid Polym. Sci.* **1984**, *262*, 489; b) O. Kamo, K. Matsushita, Y. Terada, T. Yoshida, H. Okabayashi, *Chem. Scr.* **1984**, *23*, 189; c) C. A. Martin, L. M. Magid, *J. Phys. Chem.* **1981**, *85*, 3938; d) J. Zhang, J. Jonas, *J. Phys. Chem.* **1994**, *98*, 6835.
[15] a) T. Umecky, M. Kanakubo, Y. Ikushima, *Fluid Phase Equilib.* **2005**, *228*, 329; b) K. R. Harris, M. Kanakubo, L. A. Woolf, *J. Chem. Eng. Data* **2007**, *52*, 1080; c) M. Kanakubo, K. R. Harris, N. Tsuchihashi, K. Ibuki, M. Ueno, *J. Phys. Chem. B* **2007**, *111*, 2062.
[16] Although the mechanism of the reduction reaction is not clear at the present stage, the amine ligand can possibly act as a reducing agent and the reduction process is accelerated by temperature and light.
[17] For example, see: a) C. W. Scheeren, G. Machado, S. R. Teixeira, J. Morais, J. B. Domingos, J. Dupont, *J. Phys. Chem. B* **2006**, *110*, 13011; b) A. Taubert, Z. Li, *Dalton Trans.* **2007**, 723.
[18] A. J. Bruno, S. Chaberek, A. E. Martell, *J. Am. Chem. Soc.* **1956**, *78*, 2723.

Received: November 9, 2007
Revised: February 12, 2008
Published online: April 9, 2008

 © 2008 Wiley-VCH Verlag GmbH & Co. KGaA, Weinheim